Thermochimica Acta, 219 (1993) 215–224
Elsevier Science Publishers B.V., Amsterdam

Preparation and thermal decomposition of solid state compounds of 4-methoxybenzylidenepyruvate and trivalent lanthanides and yttrium

L.C.S. de Oliveira, C.B. Melios, M. Spirandeli Crespi, C.A. Ribeiro and M. Ionashiro *

Instituto de Química, Universidade Estadual Paulista, Araraquara, São Paulo, C.P. 355, CEP 14800-900 (Brazil)

(Received 8 September 1992)

Abstract

Solid state compounds were prepared of Ln–4-MeO-BP, where Ln is a trivalent lanthanide (except promethium) or yttrium, and 4-MeO-BP is 4-methoxybenzylidenepyruvate. Thermogravimetry–derivative thermogravimetry (TG–DTG), differential scanning calorimetry (DSC) and other methods of analysis have been used to characterize and to study the thermal stability and thermal decomposition of these compounds.

INTRODUCTION

Investigations in aqueous solution of several metal ion complexes with 4-MeO-BP 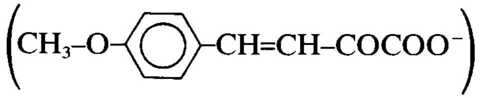 4-methoxybenzylidenepyruvate have mainly reported the thermodynamic stability (β_1) and spectroscopic parameters ($\varepsilon_{1\text{max}}, \lambda_{\text{max}}$) of 1:1 species [1–3]. We found no references concerning the preparation of solid state complexes of trivalent lanthanides and yttrium with 4-MeO-BP.

The present work investigates the solid state compounds of Ln–4-MeO-BP, their stoichiometry, thermal stability and thermal decomposition, using complexometric methods, TG–DTG, DSC and X-ray diffraction powder patterns.

EXPERIMENTAL

The complex Na–4-MeO-BP was prepared as described in ref. 4. Lanthanide(III) and yttrium(III) chlorides were prepared as described [5].

---

* Corresponding author.

The solid state complexes of trivalent lanthanides and yttrium with 4-MeO-BP were prepared by the stoichiometric reaction of the aqueous solution of Na–4-MeO-BP with an aqueous solution of the corresponding lanthanide or yttrium chloride. The precipitates obtained were washed until elimination of chloride ions, filtered and dried in Whatman No. 42 filter papers, and stored in a desiccator over anhydrous calcium chloride.

After igniting the compounds to the respective oxide, the lanthanide(III) and yttrium(III) ion contents were determined by complexometric titration with standard EDTA solution using xylenol orange as indicator [6], and from the TG curves. The water and 4-MeO-BP were determined from the TG curves.

The TG–DTG and DSC curves were obtained using a Mettler TA-4000 thermoanalyser system with an air flux of ≈150 ml min^{-1}, a heating rate of 5°C min^{-1} and with samples weighing about 7 mg. An alumina crucible with a perforated cover was used for the TG–DTG curves and an aluminium crucible with a perforated cover was used for the DSC curves.

Diffraction patterns were obtained as previously described [7].

RESULTS AND DISCUSSION

Table 1 presents the analytical and thermoanalytical (TG) results of the prepared compounds whose composition is represented by the formula $Ln(4\text{-}MeO\text{-}BP)_3 \cdot nH_2O$.

TABLE 1

Analytical and thermoanalytical (TG) results

Compound	Ln (%)			L (%)		Water (%)	
	Calcd.	EDTA	TG	Calcd.	TG	Calcd.	TG
$La(L)_3 \cdot 2H_2O$	17.57	17.22	17.90	79.39	79.01	4.56	4.94
$Ce(L)_3 \cdot 1.5H_2O$	17.90	17.91	18.05	78.01	77.85	3.45	3.26
$Pr(L)_3 \cdot 1.5H_2O$	17.98	18.28	18.18	78.27	78.03	3.45	3.43
$Nd(L)_3 \cdot H_2O$	18.54	18.00	18.73	78.37	78.78	2.32	2.71
$Sm(L)_3 \cdot H_2O$	19.18	19.09	19.61	77.76	77.37	2.30	2.78
$Eu(L)_3 \cdot 2H_2O$	19.35	19.47	19.13	77.60	77.85	4.59	4.23
$Gd(L)_3 \cdot 1.5H_2O$	19.66	19.53	20.04	77.34	76.91	3.38	3.81
$Tb(L)_3 \cdot 1.5H_2O$	19.84	19.91	19.99	76.67	76.49	3.37	3.47
$Dy(L)_3 \cdot H_2O$	20.41	20.72	20.66	76.57	76.29	2.26	2.50
$Ho(L)_3 \cdot H_2O$	20.66	20.37	20.99	76.34	75.96	2.26	2.72
$Er(L)_3 \cdot 1.5H_2O$	20.65	20.86	20.67	76.38	76.36	3.34	3.45
$Tm(L)_3 \cdot 1.5H_2O$	20.82	20.71	21.14	76.23	75.86	3.33	3.35
$Yb(L)_3 \cdot 1.5H_2O$	21.22	21.00	21.02	75.84	76.02	3.31	3.62
$Lu(L)_3 \cdot 1.5H_2O$	21.40	21.12	21.63	75.66	75.41	3.33	3.55
$Y(L)_3 \cdot 1.5H_2O$	12.15	12.18	12.41	84.58	84.26	3.69	4.00

Key: Ln means lanthanides and yttrium; L means 4-methoxybenzylidenepyruvate.

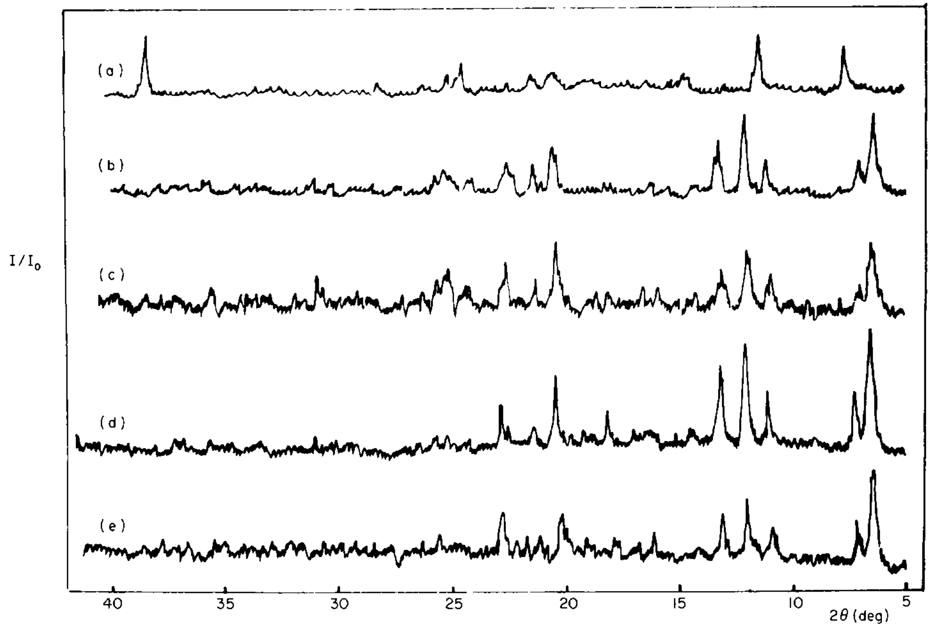

Fig. 1. X-ray powder diffraction patterns of (a) $LaL_3 \cdot 2H_2O$; (b) $CeL_3 \cdot 1.5H_2O$; (c) $PrL_3 \cdot 1.5H_2O$; (d) $NdL_3 \cdot H_2O$ and (e) $SmL_3 \cdot H_2O$. (L is 4-MeO-BP.)

The X-ray powder diffraction patterns, Fig. 1, show that the La–Sm complexes tend towards a crystalline structure, with, except for the lanthanum compound, evidence for formation of an isomorphous series. The diffraction patterns for the Eu–Lu and yttrium compounds indicate an amorphous structure.

The TG–DTG curves are shown in Fig. 2. These curves show mass losses in three or four steps between 80 and 890°C. The first mass loss up to ≈170°C is ascribed to the dehydration: the TG–DTG curves of the lanthanum compound, Fig. 2(a), shows dehydration in two consecutive steps; for the other compounds the dehydration occurs in one step.

After the dehydration, the mass losses observed above 180°C for La–Tb, Fig. 2(a) to 3 h, above 160°C for Dy, Fig. 2(i), and above 165°C for Ho–Lu and Y, Fig. 2(j)–(o), are due to the thermal decomposition of the anhydrous compounds; these take place in two or three consecutive steps with partial losses characteristic of each compound.

In the last step for all the compounds, except for cerium, the TG–DTG curves suggest the thermal decomposition of the intermediate compounds $La_2(CO_3)_3$, $Ln_2O(CO_3)_2$ or $Ln_2O_2CO_3$. Tests with hydrochloric acid solution on samples heated up to the temperatures given on the TG–DTG curves, indicated the presence of these intermediate compounds, together with a small quantity of carbon residue. For the cerium compound, Fig. 2(b), no intermediate is formed, probably because of the oxidation reaction of

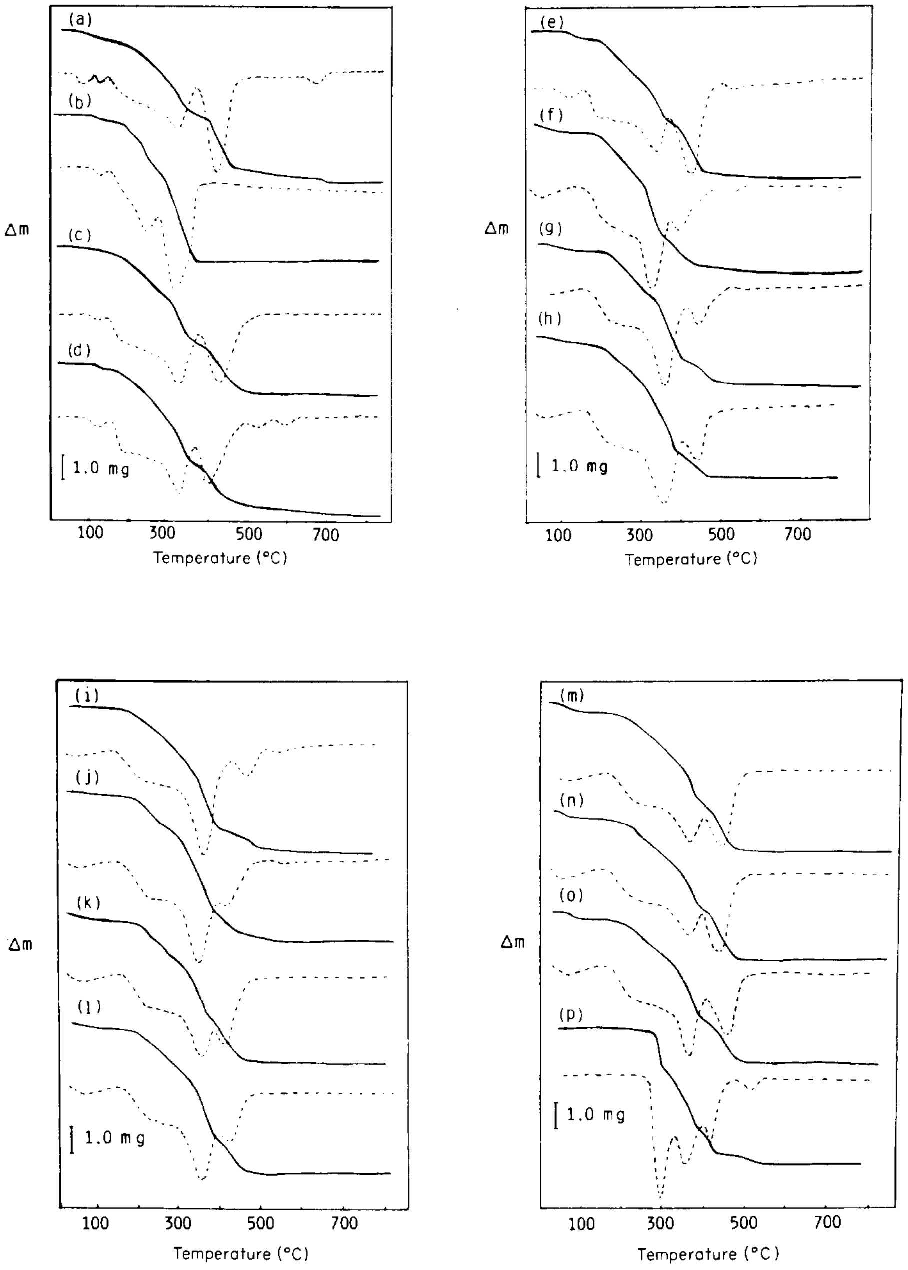

Fig. 2. TG-DTG curves of (a) $LaL_3 \cdot 2H_2O$ (7.188 mg); (b) $CeL_3 \cdot 1.5H_2O$ (7.109 mg); (c) $PrL_3 \cdot 1.5H_2O$ (7.165 mg); (d) $NdL_3 \cdot H_2O$ (7.128 mg); (e) $SmL_3 \cdot H_2O$ (7.133 mg); (f) $EuL_3 \cdot 2H_2O$ (7.145 mg); (g) $GdL_3 \cdot 1.5H_2O$ (7.145 mg); (h) $TbL_3 \cdot 1.5H_2O$ (7.155 mg); (i) $DyL_3 \cdot H_2O$ (7.039 mg); (j) $HoL_3 \cdot H_2O$ (7.196 mg); (k) $ErL_3 \cdot 1.5H_2O$ (7.154 mg); (l) $TmL_3 \cdot 1.5H_2O$ (7.136 mg); (m) $YbL_3 \cdot 1.5H_2O$ (7.132 mg); (n) $LuL_3 \cdot 1.5H_2O$ (7.185 mg); (o) $YL_3 \cdot 1.5H_2O$ (7.199 mg); (p) NaL (7.190 mg). L is 4-MeO-BP; heating rate, 5°C min^{-1}; air flux, 150 ml min^{-1}.

TABLE 2

Mass losses and temperature ranges corresponding to the partial thermal decomposition of the compounds $Ln(L)_3 \cdot nH_2O$, where Ln means lanthanide and L means 4-methoxybenzylidenepyruvate

Compound	Δm (mg)	ΔT (°C)	Partial loss of the compound	TG (%)	Calcd. (%)
$LaL_3 \cdot 2H_2O$	0.193	80–110	$1H_2O$	2.69	2.28
	0.162	110–160	$1H_2O$	2.25	2.28
	2.893	180–400	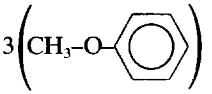	40.25	40.66
	1.848	400–470	Remainder of the ligand with formation of carbonate	25.71	25.83
	0.583	470-720	$1.5CO_2$	8.11	8.35
$CeL_3 \cdot 1.5H_2O$	0.232	120–160	$1.5H_2O$	3.26	3.45
	2.211	180–305	$3(CH_3\text{–}O\text{–})$, 2 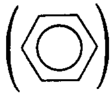	31.10	31.34
	3.091	305–410	Remainder of the ligand	43.48	43.22
$PrL_3 \cdot 1.5H_2O$	0.246	120–165	$1.5H_2O$	3.43	3.45
	3.407	180–390	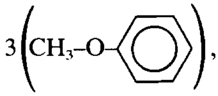, 2(–CH=CH–)	47.55	47.67
	1.732	390–490	Remainder of the ligand with formation of dioxycarbonate	24.17	24.35
	0.206	490–600	$0.5CO_2$	2.88	2.81
$NdL_3 \cdot H_2O$	0.193	120–155	$1H_2O$	2.71	2.32
	3.406	180–385	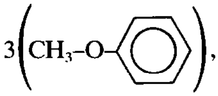, 2(–CH=CH–)	47.78	48.02
	1.570	385–485	Remainder of the ligand with formation of oxycarbonate	22.03	22.38
	0.408	485–715	$1CO_2$	5.72	5.65
$SmL_3 \cdot H_2O$	0.198	110–150	$1H_2O$	2.78	2.30
	3.129	180–390	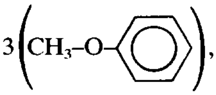, (–CH=CH–)	43.87	44.32
	1.993	390–500	Remainder of the ligand with formation of dioxycarbonate	27.94	28.33
	0.199	500–770	$0.5CO_2$	2.79	2.80

TABLE 2 (continued)

Compound	Δm (mg)	ΔT (°C)	Partial loss of the compound	TG (%)	Calcd. (%)
$EuL_3 \cdot 2H_2O$	0.302	45–140	$2H_2O$	4.23	4.59
	3.874	180–365	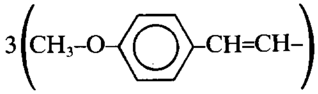	54.30	54.44
	1.007	365–495	Remainder of the ligand with formation of oxycarbonate	14.09	14.26
	0.373	495–750	$1CO_2$	5.22	5.60
$GdL_3 \cdot 1.5H_2O$	0.272	45–110	$1.5H_2O$	3.81	3.38
	4.071	180–395	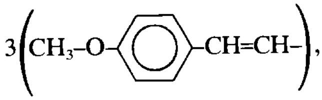, 2CO	56.96	56.95
	0.969	395–495	Remainder of the ligand with formation of dioxycarbonate	14.00	14.26
	0.183	495–755	$0.5CO_2$	2.56	2.75
$TbL_3 \cdot 1.5H_2O$	0.248	45–120	$1.5H_2O$	3.47	3.37
	4.052	180–390	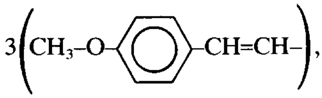, CO_2	56.71	56.94
	0.996	390–455	Remainder of the ligand with formation of dioxycarbonate	13.92	14.23
	0.177	455–775	$0.5CO_2$	2.47	2.75
$DyL_3 \cdot H_2O$	0.176	45–125	$1H_2O$	2.50	2.26
	4.261	160–405	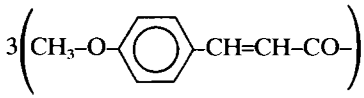	60.53	60.74
	0.728	405–520	Remainder of the ligand with formation of dioxycarbonate	10.34	10.81
	0.206	520–895	$0.5CO_2$	2.93	2.77
$HoL_3 \cdot H_2O$	0.196	45–120	$1H_2O$	2.72	2.26
	4.086	165–395	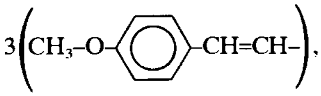, CO	56.78	57.05
	1.007	395–465	Remainder of the ligand with formation of dioxycarbonate	13.99	14.28
	0.178	465–815	$0.5CO_2$	2.47	2.75

TABLE 2 (continued)

Compound	Δm (mg)	ΔT (°C)	Partial loss of the compound	TG (%)	Calcd. (%)
$ErL_3 \cdot 1.5H_2O$	0.247	45–120	$1.5H_2O$	3.45	3.34
	3.779	165–400	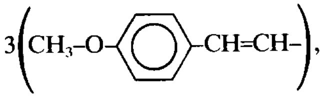 , CO	52.82	52.79
	1.261	400–460	Remainder of the ligand with formation of dioxycarbonate	17.63	17.54
	0.176	460–845	$0.5CO_2$	2.71	2.46
$TmL_3 \cdot 1.5H_2O$	0.239	45–120	$1.5H_2O$	3.35	3.33
	3.780	165–390	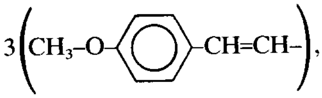 , CO	52.97	52.68
	1.223	390–455	Remainder of the ligand with formation of dioxycarbonate	17.14	17.50
	0.171	455–775	$0.5CO_2$	2.40	2.71
$YbL_3 \cdot 1.5H_2O$	0.258	45–120	$1.5H_2O$	3.62	3.31
	3.270	165–390	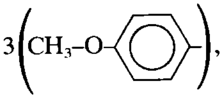 , (CH=CH–)	45.85	45.79
	1.724	390–460	Remainder of the ligand with formation of dioxycarbonate	24.18	24.15
	0.170	460–770	$0.5CO_2$	2.38	2.70
$LuL_3 \cdot 1.5H_2O$	0.255	45–125	$1.5H_2O$	3.55	3.31
	3.248	165–400	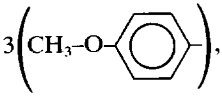 , 2(CH=CH–)	45.22	45.68
	1.914	400–465	Remainder of the ligand with formation of a mixture of oxide and dioxycarbonate	25.18	25.32
	0.105	465–830	$0.25CO_2$	1.46	1.36
$YL_3 \cdot 1.5H_2O$	0.287	45–125	$1.5H_2O$	4.00	3.69
	3.895	165–395	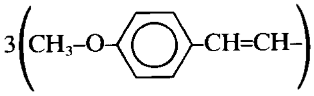	54.26	54.62
	1.742	395–480	Remainder of the ligand with formation of a mixture of oxide and dioxycarbonate	24.27	24.46
	0.125	480–835	$0.3CO_2$	1.74	1.80

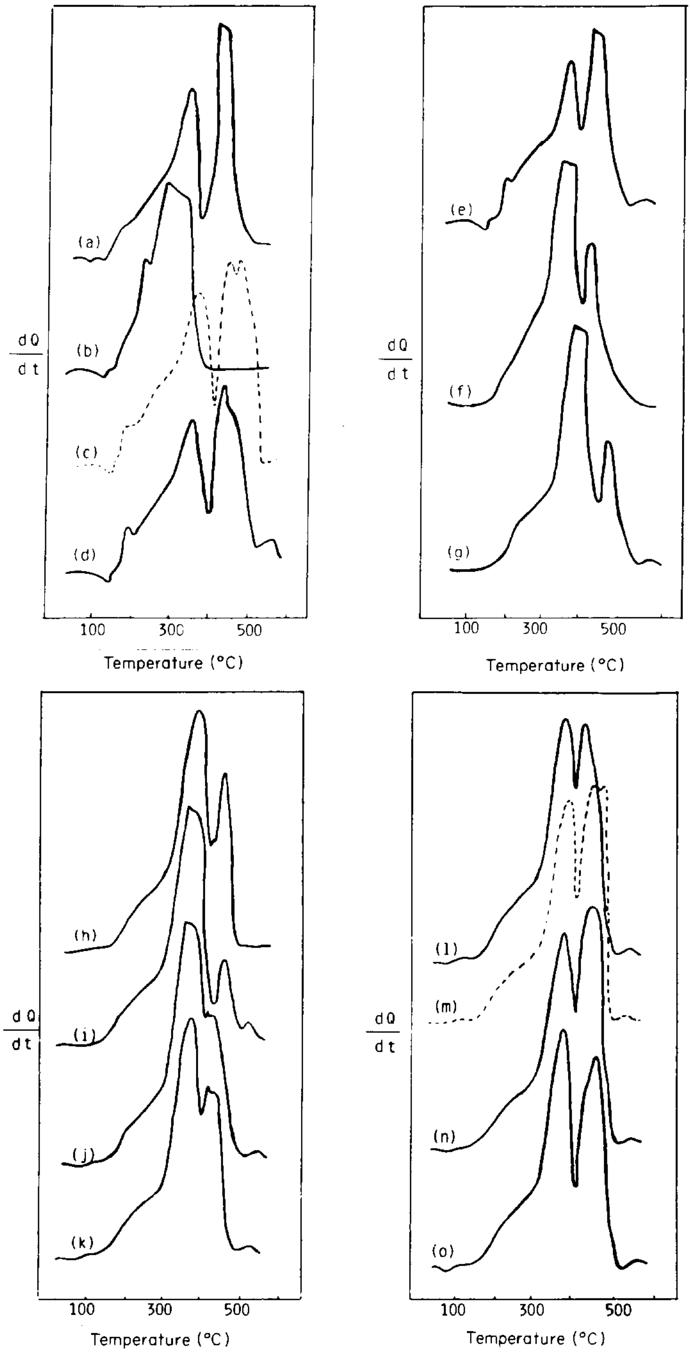

Fig. 3. DSC curves of (a) $LaL_3 \cdot 2H_2O$ (7.081 mg); (b) $CeL_3 \cdot 1.5H_2O$ (7.036 mg); (c) $PrL_3 \cdot 1.5H_2O$ (7.165 mg); (d) $NdL_3 \cdot H_2O$ (7.133 mg); (e) $SmL_3 \cdot H_2O$ (7.145 mg); (f) $EuL_3 \cdot H_2O$ (7.145 mg); (g) $GdL_3 \cdot 1.5H_2O$ (7.145 mg); (h) $TbL_3 \cdot 1.5H_2O$ (7.155 mg); (i) $DyL_3 \cdot H_2O$ (7.196 mg); (j) $HoL_3 \cdot H_2O$ (7.196 mg); (k) $TmL_3 \cdot 1.5H_2O$ (7.154 mg); (l) $ErL_3 \cdot 1.5H_2O$ (7.136 mg); (m) $YbL_3 \cdot 1.5H_2O$ (7.132 mg); (n) $LuL_3 \cdot 1.5H_2O$ (7.185 mg); (o) $YL_3 \cdot 1.5H_2O$ (7.084 mg). L is 4-MeO-BP; heating rate, 5°C min^{-1}; air flux, 150 ml min^{-1}.

Ce(III) to Ce(IV), as has been observed for other cerium(III) compounds [7,8].

The mass losses, temperature ranges and the probable partial losses observed in each step of the TG–DTG curves are shown in Table 2.

The DSC curves are shown in Fig. 3. These curves show endothermic and exothermic peaks that all accord with the mass losses observed in the TG–DTG curves up to 600°C.

For the La–Sm compounds, Fig. 3(a)–(e) whose TG–DTG curves show dehydration below 165°C, the corresponding DSC curves exhibit endothermic peaks at ≈130°C. For the other compounds, except for yttrium whose TG–DTG curves show dehydration below 120°C, the corresponding DSC curves show that the dehydration occurs by a slow endothermic process without the appearance of definite peaks. This behaviour is in accordance with the TG–DTG curves and is probably due to the structure of these compounds, as already observed from the X-ray diffraction patterns.

The broad exotherms observed for all compounds, with two or three peaks between ≈150 and 550°C, are attributed to the thermal decomposition of the anhydrous compounds, where the oxidation of the organic matter takes place in consecutive stages; this is in agreement with the TG–DTG curves.

The small exothermic peaks observed for some compounds at ≈560°C, Fig. 3(d), (e), (g), and (i)–(o), are attributed to the simultaneous final oxidation of the carbonaceous material resulting from the thermal decomposition process (exothermic) and the thermal decomposition of the intermediate oxy- or dioxycarbonate (endothermic), yielding the small exothermic peak.

CONCLUDING REMARKS

The X-ray powder patterns verified that the lighter lanthanide compounds tend towards a crystalline structure and the heavier lanthanide compounds indicate an amorphous structure.

The TG–DTG and DSC curves established the stoichiometry of the compounds in the solid state and also provided information about the thermal stability and thermal decomposition.

ACKNOWLEDGMENTS

The authors acknowledge the FAPESP (Proc. 90/2932-4) and CNPq for the financial support.

REFERENCES

1 C.B. Melios, M. Molina and F. Martins, Ciênc. Cult. (Sao Paulo) (Supl.), 27(7) (1975) 109.
2 C.B. Melios, J.T. Souza Campos, M.A.C. Mazzeu, L.L. Campos, M. Molina and J.O. Tognolli, Inorg. Chim. Acta, 139 (1987) 163.

3 C.B. Melios, M. Ionashiro, H. Redigolo, M.H. Miyano and M. Molina, Eur. J. Solid State Inorg. Chem., 28 (1991) 291.
4 M. Raimer, J. Am. Chem. Soc., 48 (1926) 2459.
5 E. Giesbrecht, M. Perrier and W.W. Wendlandt, An. Acad. Brasil. Cienc., 34 (1962) 37.
6 M. Inoashiro, C.A.F. Graner and J. Zuanon Netto, Ecl. Quím., 8 (1983) 29.
7 M. Ionashiro, C.B. Melios, C.A. Ribeiro and M. Spirandeli Crespi, Thermochim. Acta, 168 (1990) 223.
8 L. Moscardini D'Assunção, I. Giolito and M. Ionashiro, Thermochim. Acta, 137 (1989) 319.